

# **TURBULENT DIFFUSION OF MOMENTUM AND HEAT FROM A SMOOTH, PLANE BOUNDARY WITH ZERO PRESSURE GRADIENT**

*By*

*A.C. Spengos and J.E. Cermak*



*Department of Civil Engineering*

## **FINAL REPORT - PART I EXPERIMENTAL EQUIPMENT**

The research reported in this document has been sponsored by the  
Geophysics Research Directorate of the Air Force Cambridge Research  
Center, Air Research and Development Command, under Contract  
AF19(604)-421.

**Colorado Agricultural and Mechanical College  
Fort Collins, Colorado  
August 1956**

## ABSTRACT

The experimental equipment used in an investigation of turbulent diffusion of momentum and heat from a smooth, plane boundary with zero pressure gradient is described in Part I of this Final Report.

A 10 ft long, 6 ft wide heated boundary, maintained at uniform temperature, formed part of the floor of the 6-ft square test section of a recirculating, low-velocity wind tunnel. Hot-wire anemometers were used for the measurement of mean velocities, intensities of turbulence, and turbulent shearing stress distributions in the momentum and the thermal boundary layers. Mean temperatures were measured with copper-constantan thermocouples. For the measurement of temperature fluctuations, a constant-temperature resistance thermometer was developed and used. The heat transferred from the boundary was determined from the electrical power input to the heater strips.

## CONTENTS

ABSTRACT . . . . .	i
ACKNOWLEDGEMENTS . . . . .	v
I. INTRODUCTION . . . . .	1
II. WIND TUNNEL . . . . .	2
III. HEATED BOUNDARY . . . . .	4
IV. INSTRUMENTATION . . . . .	8
Measurement of Heat Input to the Boundary . . . . .	8
Measurement of Mean Velocities . . . . .	9
Measurement of Mean Temperatures . . . . .	10
Measurement of Intensities of Turbulence and Turbulent Shearing Stress . . . . .	11
Measurement of Temperature Fluctuations . . . . .	17
Measurement of Turbulent Heat Transfer Rate . . . . .	19
REFERENCES . . . . .	20
LIST OF FIGURES . . . . .	21

## ACKNOWLEDGEMENTS

The equipment herein described was used in the experimental study presented in Part II of this Final Report. This study and a large part of the development and construction of equipment were made possible through the financial support of the Air Force Cambridge Research Center under Contract No. AF 19(604)-421.

Grateful acknowledgement is made to Mr. R. W. Sjoström for his valuable assistance in the instrumentation design and construction; to Prof. H. H. Schweizer for his participation in the early stages of the design of the equipment; and to Mr. R. T. Shen for his meticulous care in editing this report.

Acknowledgement is also made to Prof. T. H. Evans, Dean of Engineering; Dr. D. F. Peterson, Head of the Department of Civil Engineering; and to Dr. M. L. Albertson, Professor of Civil Engineering, for their support and administrative supervision.

## I. INTRODUCTION

For the past four years an experimental investigation on the turbulent diffusion of momentum and heat has been conducted in the wind tunnel facilities of Colorado A and M College. This investigation was confined to the case of flow of air over a heated, smooth, and plane boundary with zero pressure gradient. In a previous report (9)<sup>1</sup> a brief description of the experimental equipment has been included. However, since considerable time and effort have been devoted to the development of this equipment, a detailed description and discussion of it seems justifiable. This is particularly true when the scarcity of published information regarding previously conducted investigations is taken into consideration.

Along with the description of the equipment, an attempt was made to indicate possible improvements that might be introduced to future investigations.

The equipment used in this investigation consisted of (a) the recirculating wind tunnel, (b) the heated boundary, and (c) the associated instrumentation. Instruments were constructed for the measurement of heat input to the boundary, mean velocity, mean temperature, and turbulent shearing stress distributions in the boundary layer, as well as root-mean-square fluctuations of the velocity and of the temperature.

In Part II of this Final Report, an analysis and discussion of the data obtained during the experimental investigation is presented.

---

<sup>1</sup> The number refers to the bibliographical entry in the REFERENCES.

## II. WIND TUNNEL

The recirculating wind tunnel shown in Fig. 1 has a 6 ft square test section 30 ft in length. The four-bladed propeller was driven by a 50-HP gasoline engine geared directly to the shaft of the propeller, and a 150-HP marine diesel engine coupled to the propeller shaft through V-belts and sheaves. This dual drive system made it possible to vary the velocity in the test section from 3 fps to about 50 fps. For the lower range of velocities the gasoline engine was used. When necessary the velocity was further reduced by the use of cheese-cloth extending over the entire flow area and fastened to the turning vanes located at the downstream end of the test section.

The distribution of the ambient air velocity, both along and perpendicular to the longitudinal axis of the test section, was found to have a variation of about  $\pm 2$  per cent from the mean value except within the wall boundary layers. The pressure distribution along the longitudinal axis of the test section was measured with a Pitot tube and Whalen gage arrangement. The variation of this pressure was found to be within 2 per cent of the mean value as shown in Fig. 2. The turbulence intensity level of the ambient air stream was about 1 per cent for the velocity range used in the experimental investigation.

Although the amount of heat transferred from the heated boundary was varied from about 4500 watts to 6000 watts, the ambient temperature of the recirculating air was not affected appreciably. The mixing effected by the propeller action, and the heat transferred through the tunnel walls, particularly through the floor of the test

section immediately downstream from the heated boundary where actual inversion occurred, contributed toward maintaining a relatively constant ambient air temperature.

### III. HEATED BOUNDARY

A schematic diagram of the test section is shown in Fig. 3. The dynamically smooth and heated boundary, over which the momentum and thermal boundary layers developed, was 6 ft wide, 10 ft long, and formed part of the floor of the test section.

In order to stimulate the growth of the dynamic boundary layer, a 1.5 ft wide strip of  $\frac{1}{8}$ -in. gravel was laid across the floor of the test section 1.67 ft upstream from the heated boundary. It has been found by other investigators (5) that such an artificial method of thickening the boundary layer is advantageous in cases where the test section is not long enough for the normal growth of the boundary layer into a fully turbulent state.

There is some question as to whether such an artificially induced boundary layer is similar in all respects to one developed without the use of a stimulator. Although the mean velocity profiles might indicate the development of a fully-turbulent boundary layer, the turbulent shearing stress and the turbulent intensities distributions might still be different from those of a fully-turbulent boundary layer developed without a stimulator. If such an artificial method of thickening the boundary layer could be avoided or if more comparative measurements of turbulent boundary layer characteristics for natural and artificially stimulated growth were available, the experimental results would be free from such doubts.

The construction details of the heated boundary are shown in Fig. 4. This consisted of a  $\frac{1}{2}$  in. thick aluminum plate on top of which the heater strips, covering the entire surface, were mounted.



The  $\frac{1}{2}$ -in. aluminum plate provided a sturdy support for the heater strips, and the heat stored in it contributed in maintaining a constant temperature over the entire surface of the heated boundary. Although a servomechanism was provided to keep the surface temperature within 2°F of a predetermined value and eliminate effects of line voltage fluctuations and small ambient velocity changes, the servomechanism was found unnecessary during the preliminary runs and its use was discontinued.

The heater strips, comprising the 23 electrically isolated heating elements, consisted of  $\frac{1}{16}$ -in. aluminum supporting plates of varying width, on which a thin layer of carbon was placed. The top and the bottom sides of the carbon layer were electrically insulated by several layers of silicone varnish. The physical dimensions and electrical characteristics of each of the 23 heater strips are given in Table I. The bus bars connected to the main powerstat, as well as the electrical circuit for the No. 1 heater strip, are shown in Fig. 5. The electrical connections for the remaining 22 heater strips were identical. A neon lamp was used as a pilot light for each strip.

Although the use of a thin carbon layer as a heating element was found satisfactory, sparking due to possible discontinuities in the layer reduced its useful life. Recently, thin sheets of high-resistance metals have been made available commercially. These might provide more durable heating elements at considerably less cost.

The total electrical power input to the heated boundary was adjusted by the use of a powerstat. A rheostat connected in series with each heater strip provided the proper power adjustment for each

strip so that a surface of uniform temperature was obtained for a given ambient velocity and temperature. For temperature differences between the ambient air and the heated boundary of approximately 100°F, the variation of the temperature over the entire surface was within 6°F from the mean.

Under the  $\frac{1}{2}$ -in. aluminum plate a 4 in. thick layer of glass wool provided adequate thermal insulation. Measurements have shown that only 2 per cent of the heat input was dissipated from surfaces other than the top of the heated boundary over which the thermal boundary layer developed.

Figs. 6, 7, 8, and 9 show various views of the test section, heated boundary, and electrical control panel.

TABLE I HEATER STRIP CHARACTERISTICS

Strip No.	Strip Width in.	Strip Length in.	Strip Res. ohms	Fuse amps	Rheostat ohms
1	0.5	70.5	225	1.5	25.0
2	1.0	"	185	1.5	15.0
3	1.0	"	225	1.5	25.0
4	1.0	"	210	1.5	35.0
5	2.0	"	130	3.0	22.0
6	2.0	"	130	3.0	25.0
7	2.0	"	128	3.0	25.0
8	2.0	"	136	3.0	22.0
9	4.0	"	68	4.0	10.0
10	4.0	"	77	4.0	15.0
11	4.0	"	68	3.0	15.0
12	8.0	"	48	6.0	7.5
13	8.0	"	43	6.0	7.5
14	8.0	"	47	6.0	7.5
15	8.0	"	57	5.0	7.5
16	8.0	"	48	5.0	7.5
17	8.0	"	51	5.0	7.5
18	8.0	"	48	5.0	7.5
19	8.0	"	44	5.0	7.5
20	8.0	"	56	5.0	7.5
21	8.0	"	64	5.0	7.5
22	8.0	"	50	5.0	7.5
23	8.0	"	54	5.0	7.5

#### IV. INSTRUMENTATION

The apparatus used for the collection of data consisted of meters for the measurement of heat power input to the boundary, and the instruments for the indication of mean velocity and temperature, intensity of turbulence, turbulent shearing stress, and temperature fluctuation.

The sensing elements of the above-mentioned instruments were mounted on a carriage located 3 ft above the floor of the test section and supported by rails fastened to the tunnel walls. Two electric motors, with their controls located outside the test section, were used to control lateral and vertical motions of the sensing elements. This arrangement made it possible to locate the sensing elements at any desired point above the heated boundary. The error in the vertical coordinate values was within 0.005 in.

##### Measurement of Heat Input to the Boundary

The electrical power input to each heater strip was measured with an ammeter and voltmeter. As shown in Fig. 5 for strip No. 1, a three-circuit, make-break jack located on the control panel in series with the heater strips provided a convenient outlet for the connection of the ammeter-voltmeter arrangement shown in the same figure.

The total power input to the boundary was obtained by totaling the inputs to the 23 electrically isolated heater strips.

### Measurement of Mean Velocities

The mean velocity profiles in the boundary layer, as well as the ambient velocity, were measured by means of a platinum constant-temperature hot-wire anemometer 0.4 in. long and 0.001 in. in diameter. The circuit of this anemometer is shown in Fig. 10. For changes in mean velocity, the balance of the Wheatstone bridge, indicated by the galvanometer connected across it, was restored manually by adjusting the current flowing through the bridge. Two rheostats, one for coarse and the other for fine adjustment, connected in series with the battery, were used for this adjustment. The milliammeter, in series with the bridge and the battery, indicated the mean velocity of the air.

The large time constant of the hot-wire, due to its mass, and of the current indicating meter reduced considerably the response of the anemometer to velocity fluctuations and made the measurement of the mean velocity possible in the boundary layer where large fluctuations existed.

Compensation of the hot-wire for mean temperature variations in the thermal boundary layer was accomplished by mounting a resistance element on the same probe with the hot-wire. This element formed the branch of the bridge opposite to that of the hot-wire and consisted of a coiled tungsten wire 12 in. long and 0.00031 in. in diameter. Fig. 11b shows the probe on which the hot-wire and the compensator were mounted. The initial balancing of the bridge (for the case without air flow) was accomplished by adjusting the variable resistance in the upper left branch, Fig. 10. Although the above method of compensation is a common practice and is also theoretically justifiable, no means was available for an experimental proof of its effectiveness.

Preceding the collection of data, the relation between total bridge current and air velocity, for constant temperature operation of the hot-wire, was obtained with a rotating arm calibration arrangement. Because of the relatively high operating temperature of the hot-wire, about 1000°F, small changes of the ambient air temperature did not affect its calibration. However, as a result of the high operating temperature, thermal radiation effects were observed for distances between the hot-wire and the heated boundary smaller than 0.050 in. The mean velocity profiles obtained by using the above instrument could be duplicated within a 3 per cent variation.

#### Measurement of Mean Temperatures

The mean temperature distribution in the thermal boundary layer, the temperature of the ambient air, and that of the surface of the heated boundary were measured with copper-constantan thermocouples, 0.010 in. in diameter, which were connected to a standard Honeywell recording type potentiometer. Because of the relatively small size of the thermocouples and the large temperature fluctuations in the thermal boundary layer, a Weston Model 808 integrator was used for the correct measurement of the mean value of the temperature. Time intervals of approximately  $\frac{1}{2}$ -minute duration were used.

The thermocouple probe for the measurement of the temperature distribution in the boundary layer and the temperature of the surface of the boundary is shown in Fig. 11c. It was observed in this investigation, as well as in others (7), that a configuration of the leads in the immediate vicinity of the thermocouple, such as shown in Fig. 11c., reduces considerably the error due to heat conduction through the leads.

Originally it was planned to measure the surface temperature of the heated boundary with 69 thermocouples attached to the surface, three to each heater strip, and located along the centerline and sides of the boundary. However, during the preliminary runs it was found that owing to the size of the thermocouples, 0.010 in. in diameter, and the uneven thickness of the layer of glue, the thermocouples protruded unevenly into the thermal boundary layer, and therefore indicated temperatures other than those of the surface. To overcome this difficulty, a thermocouple attached on the end of a probe free to slide over the surface was used. With this method, although the indicated temperatures were lower than the actual, owing to conduction losses through the probe, the error introduced was the same for all points of measurement. It was thus possible to obtain a uniform temperature over the entire surface by separate adjustment of the heat input to the strips. The actual temperature of the surface of the heated boundary was measured with the thermocouple shown in Fig. 11c. The spring action of the leads of this thermocouple and the somewhat flattened junction ensured good contact with the surface; there the thermocouple assumed the temperature of the surface.

#### Measurement of Intensities of Turbulence and Turbulent Shearing Stress

The vertical and the horizontal intensities of turbulence and the turbulent shearing stress in the boundary layer were measured with a pair of crossed hot-wire anemometers of the constant temperature type (3). The length of each of the tungsten hot-wires was 0.1 in. and the diameter 0.00031 in. Compensation for mean temperature variations in

the thermal boundary layer was accomplished by mounting a resistance element on the same probe with the hot-wire. This element, with a variable resistance in series with it, constituted the branch of the Wheatstone bridge opposite to that of the hot-wire. The compensator consisted of tungsten wire 2 in. long and 0.00031 in. in diameter. The variable resistance in series with the compensator made possible the initial balancing of the bridge. In Fig. 11d, the probe for the two crossed hot-wires and their respective temperature compensators are shown. The effect of the fluctuations of the air temperature in the thermal boundary layer was minimized by the relatively large operating temperature of the hot-wires, approximately 500°F. The two Wheatstone bridges with the associated current-control circuits are shown in Figs. 12 and 13. The adding and subtracting circuit, and the turbulence amplifier and root-mean-square indicator are shown in Figs. 14 and 15 respectively. The frequency response of both the hot-wire and the associated electronic circuitry mentioned above was about 5000 cps.

The wall shearing stress was determined by extrapolation of the turbulent shearing stress distribution in the boundary layer. For the case of neutral stability, accurate results were obtained by this method because of the constant value of the turbulent shearing stress near the boundary. However, in the case of flow with lapse rates the shearing stress near the boundary changed rather rapidly and the extrapolated value could not be defined as accurately. A shear meter embedded in the heated boundary, although it might introduce a discontinuity in the uniform temperature of the surface, would be desirable in order to determine the wall shearing stress more accurately.



The mathematical derivation of the equations relating the hot-wire current to the flow properties, as well as the limitations of these equations, are described in References (1) and (4). The root-mean-square value of the horizontal intensity of turbulence was computed from the equation

$$\frac{u'}{U} = \frac{A}{2nI} \cdot \frac{G}{G_t} (I_t)_{\text{add}} , \quad (1)$$

where  $u'$  is the rms value of the horizontal fluctuating component of velocity;

$U$  is the mean local velocity in the horizontal direction;

$A$  ,  $n$  ,  $G$  , and  $G_t$  are calibration constants;

$I$  is the reading of the bridge meter; and

$(I_t)_{\text{add}}$  is the reading of the rms meter  $I_t$  of the indicator circuit when the signals from the hot-wires are added instantaneously through the adding circuit.

Similarly, the root-mean-square value of the vertical intensity of turbulence was computed from the equation

$$\frac{v'}{U} = \frac{A}{2nI} \cdot \frac{G}{G_t} (I_t)_{\text{sub}} , \quad (2)$$

where  $v'$  is the rms value of the vertical fluctuating component of velocity;

$(I_t)_{\text{sub}}$  is the reading of the rms meter  $I_t$  of the indicator circuit when the signals from the two hot-wires are subtracted instantaneously through the subtracting circuit; and

$U$  ,  $A$  ,  $n$  ,  $G$  ,  $G_t$  , and  $I$  are the same as for Eq 1.

The turbulent shearing stress was computed by using the equation

$$\frac{\overline{uv}}{U^2} = \frac{A^2}{4n^2I^2} \cdot \frac{G^2}{G_t^2} \left[ (I_t)_1^2 - (I_t)_2^2 \right] , \quad (3)$$

where  $\overline{uv} = \frac{\tau}{\rho}$  , the turbulent shearing stress divided by air density;

$(I_t)_1$  is the reading of the rms meter  $I_t$  of the indicator circuit for the signal of the No. 1 hot-wire;

$(I_t)_2$  is the reading of the rms meter  $I_t$  of the indicator circuit for the signal of the No. 2 hot-wire; and

$U$  ,  $A$  ,  $n$  ,  $G$  ,  $G_t$  , and  $I$  are the same as for Eq 1.

Equations 1, 2, and 3 have been developed on the assumption that the two hot-wires are identical and that they are operated at the same temperature by separate current control circuits. This implies that the calibration constants  $A$  ,  $n$  ,  $G$  , and  $G_t$  are the same for each of the two crossed hot-wires.

The calibration constant  $A$  indicates the ratio of the grid voltage to the cathode voltage of the 6L6 output tubes of the current-control circuits shown in Figs. 12 and 13, and it was determined by direct measurement of these two voltages when the hot-wire was in operation.

The calibration constant  $n$  is the exponent of the empirical equation relating the bridge meter reading  $I$  to the local mean velocity  $U$  :

$$I = b U^n . \quad (4)$$

Bq 4 is the response equation on which the derivation of Bqs 1, 2, and 3 is based and it is not usable in extrapolated form (4). This limitation

necessitated the calibration of the hot-wires for the range of velocities for which they were intended to be used. The exponent  $n$  was determined prior to the collection of data in the following manner. The crossed hot-wires were located in the ambient air stream of the test section next to the mean velocity hot-wire described previously. The air velocity was varied through the desired range, thus giving several readings of the bridge meter  $I$  and corresponding values of the mean velocity  $U$  as indicated by the mean velocity anemometer. The results were plotted on logarithmic paper and the slope  $n$  of a straight line through the points was directly determined.

The transconductance  $G$  for each of the current-control circuits was determined by calibration. This was accomplished in the following manner. The hot-wire was replaced by a fixed resistance of the same value and the bridge balanced. A calibrated external voltage, which could be varied between  $-25$  and  $-5$  volts relative to ground, was applied to the calibration jack, which automatically transferred the control grids of the 6L6 power tubes from the D-C amplifier output to the external voltage source. This external voltage  $E$  controlled the bridge current, and several readings of the bridge meter  $I$  over the upper two-thirds of the scale were obtained by varying  $E$ . The value of  $dI/dE = G$  was obtained by first plotting  $I$  vs  $\log_e E$  and determining the value of  $a_2$  in the equation  $I = a_1 - a_2 \log_e E$ , then, since  $G$  varies with  $I$ , a curve of  $G$  vs  $I$  was prepared from the equation  $G = dI/dE = a_2/E$ . By matching the 6L6 tubes of the two current-control circuits the same  $G$  vs  $I$  calibration curve was used for both hot-wires. This curve was checked at intervals of approximately

100 hours of actual operating time because of the gradual decrease of  $G$  with tube aging.

The transconductance  $G_t$  was obtained by calibration in the following manner. A calibrated alternating voltage source of rms value  $B'$  and of any convenient low audio frequency was applied to the calibration jack of the turbulence amplifier and RMS indicator circuit of Fig. 15. Values of  $I_t$  as a function of  $B'$  were then read on the  $I_t$  meter for each position of the attenuator switch.

The adding and subtracting circuit of Fig. 14, when properly adjusted, did not attenuate or amplify the two input signals and thus did not introduce any calibration constants. To adjust this circuit a signal was introduced to the balancing jack and the selector switch set at position "2", then the gain control was adjusted to give an output signal equal to the input. By setting the selector switch at position "1" and adjusting the balancing potentiometer, equality between input and output signals was again obtained. The above adjustments ensured that the signals from the No. 1 and the No. 2 hot wires remained unaltered when they passed through the circuit as well as when they were added or subtracted.

The data obtained by using the crossed hot-wire anemometers could be duplicated within a 10 per cent variation. This relatively large variation was due to needle fluctuations of the milliammeter indicating the rms values. The use of a recorder or an integrator will improve considerably the accuracy of the data by time averaging these fluctuations.

## Measurement of Temperature Fluctuations

The constant-temperature resistance thermometer shown in Fig. 16 was developed for the purpose of measuring the temperature fluctuations in the thermal boundary layer. The operation of this thermometer was based on the response characteristics of the hot-wire anemometer to both velocity and temperature fluctuations. It has been shown (2) that this response can be expressed as

$$e = \alpha \frac{t}{\Delta T} + \beta \frac{u}{U} , \quad (5)$$

where  $e$  is the voltage fluctuation across the hot-wire;

$\alpha$  and  $\beta$  are functions of the mean-velocity calibration constants and of the hot-wire operating conditions;

$t$  is the instantaneous temperature fluctuation;

$\Delta T$  is the mean temperature difference between the point of measurement and the ambient air;

$u$  is the instantaneous velocity fluctuation; and

$U$  is the mean local velocity.

By reducing the heating current flowing through the hot-wire so that  $\alpha \gg \beta$ , the wire responds primarily to temperature fluctuations, while the response to velocity fluctuations is negligible. Thus, the hot-wire becomes a simple resistance thermometer.

The current-control circuit shown in Fig. 16 is the same as that for the No. 1 hot-wire anemometer with an additional amplifier stage. The rms value of the voltage fluctuations, corresponding to the temperature fluctuations about the mean, were indicated by the  $I_t$

meter of an amplifier and RMS indicator similar to that shown in Fig. 15. In Fig. 11e, the probe of the resistance thermometer is shown. The wire proper consisted of tungsten 0.1 in. long and 0.00031 in. in diameter, and its operating temperature was slightly above that of the ambient air.

The root-mean-square value of the temperature fluctuations was computed from the equation

$$\frac{t'}{T} = \frac{A}{nI} \cdot \frac{G}{G_t} \cdot I_t \quad , \quad (6)$$

where  $t'$  is the rms value of the temperature fluctuations;

$T$  is the mean local temperature;

$I_t$  is the reading of the indicator circuit meter;

$A$  ,  $n$  ,  $G$  , and  $G_t$  are calibration constants; and

$I$  is the bridge meter reading.

The above equation was developed from the empirical equation

$$I = b T^n \quad (7)$$

in the same manner that the equation for the hot-wire anemometer was developed (1).

The calibration constant  $n$  was obtained from readings of the bridge meter and the local mean temperature determined from the mean temperature profile of the thermal boundary layer.

The calibration constants  $A$  ,  $G$  , and  $G_t$  are of the same nature as those for the crossed hot-wire anemometers and were determined by the same methods.

### Measurement of Turbulent Heat Transfer Rate

An attempt was made to obtain the turbulent heat transfer rate

$$\overline{tv} = - \frac{q}{\bar{\rho} \bar{c}_p} \quad (8)$$

by instantaneous multiplication of the signals from the resistance thermometer and the hot-wire anemometers. In the above equation,  $\overline{tv}$  is the mean of the product of instantaneous temperature and vertical velocity fluctuations,  $q$  is the heat flux, and  $\bar{\rho}$  and  $\bar{c}_p$  are the mean density and constant-pressure specific heat of air respectively. The electronic multiplier used to obtain  $\overline{tv}$  was of the quarter square type (6) utilizing the recently developed square-law tube, Raytheon type QK-329. The resistance thermometer was mounted on the same probe with the crossed hot-wire anemometer and 0.1 in. in front of them, as shown in Fig. 11d.

Unfortunately, the drift of the multiplier, particularly when the signals were of the same magnitude, and of the D-C amplifiers necessary before and after multiplication, was found to be considerable. Furthermore, a certain amount of phase shifting between the two signals was observed although capacitances were reduced to a minimum.

During several preliminary tests the values of  $\overline{tv}$  obtained were considerably lower than expected. In spite of this unsatisfactory outcome, it is possible that an improved electronic multiplier and complete elimination of phase shifting will give better results. It is hoped that in the near future, with the rapid development of computers, it will be possible to obtain commercially built multipliers of considerably more accuracy and reliability than are now available.

## REFERENCES

1. Baines, D. W. Equations for use with the constant temperature hot-wire anemometer. Iowa Institute of Hydraulic Research, State University of Iowa, 1949.
2. Corrsin, Stanley. Extended applications of the hot-wire anemometer. National Advisory Committee for Aeronautics TN 1864, April 1949.
3. Hubbard, P. G. Application of a D-C negative-feedback amplifier to compensate for the thermal lag of a hot-wire anemometer. Proceedings of the National Electronics Conference, Vol 4, 1948.
4. Hubbard, P. G. A constant-temperature hot-wire anemometer for the measurement of turbulence in air. M. S. Thesis, State University of Iowa, 1949.
5. Klebanoff, P. S. and Diehl, Z. W. Some features of artificially thickened fully developed turbulent boundary layers with zero pressure gradient. National Advisory Committee for Aeronautics TN 2475, October 1951.
6. Miller, J. A., Scott, R. B., and Soltes, A. S. A wide-band function multiplier. Electronics Research Directory, Air Force Cambridge Research Center - TR-56-107, Cambridge, Massachusetts, December 1954.
7. Scadron, M. D. and Warshawsky, I. Experimental determination of time constants and Nusselt numbers for bare-wire thermocouples in high-velocity air streams and analytic approximation of conduction and radiation errors. National Advisory Committee for Aeronautics TN 2599, January 1952.
8. Schubauer, G. B. and Klebanoff, P. S. Theory and application of hot-wire instruments in the investigation of turbulent boundary layers. National Advisory Committee for Aeronautics WR W-86, originally issued March 1946 as Advance Confidential Report JK27.
9. Spengos, A. C. Turbulent diffusion of momentum and heat from a smooth, plane boundary with zero pressure gradient. Scientific Report No. 1, Contract AF19(604) - 421, Air Force Cambridge Research Center, February 1956. (AFCRC-TN-56-259).



## LIST OF FIGURES

### Figure

- 1 Plan of wind tunnel
- 2 Pressure distribution along the centerline of test section
- 3 Schematic diagram of test section
- 4 Heated boundary
- 5 Circuit diagram of heater strip connections
- 6 View of test section looking downstream
- 7 Electrical control panel of heater strips mounted outside test section
- 8 View of test section looking upstream
- 9 Close-up view of heated boundary looking upstream
- 10 Constant-temperature hot-wire anemometer for mean velocity
- 11 Views of probes
  - a Probe assembly
  - b Mean velocity hot-wire probe
  - c Mean temperature thermocouple probe
  - d Turbulence intensities hot-wire probe
  - e Resistance thermometer probe
- 12 Constant-temperature, tungsten hot-wire anemometer No. 1  
(Current Control Circuit)
- 13 Constant-temperature, tungsten hot-wire anemometer No. 2  
(Current Control Circuit)
- 14 Adding and subtracting circuit
- 15 Turbulence amplifier and RMS indicator circuit
- 16 Constant-temperature resistance thermometer  
(Current Control Circuit)



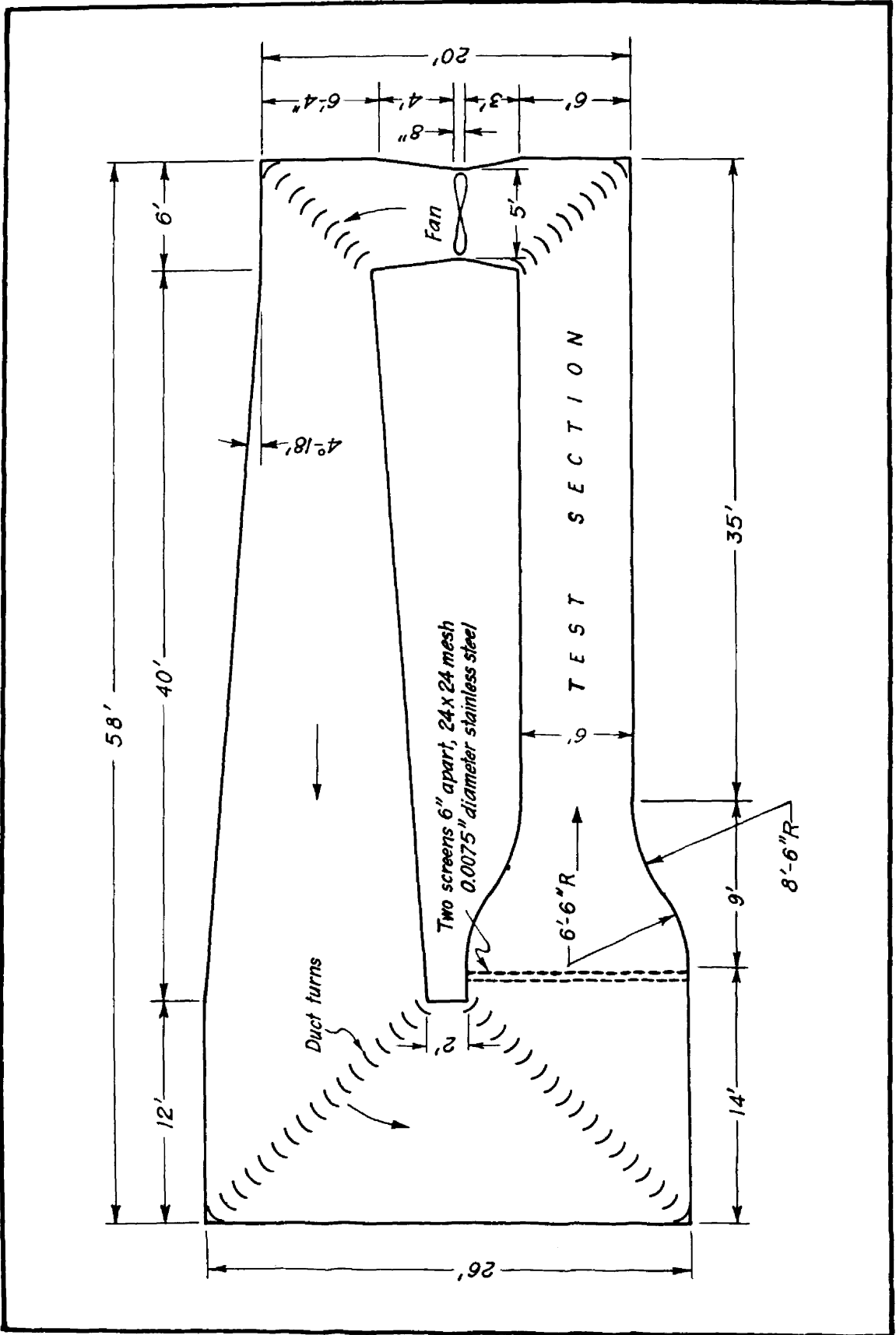
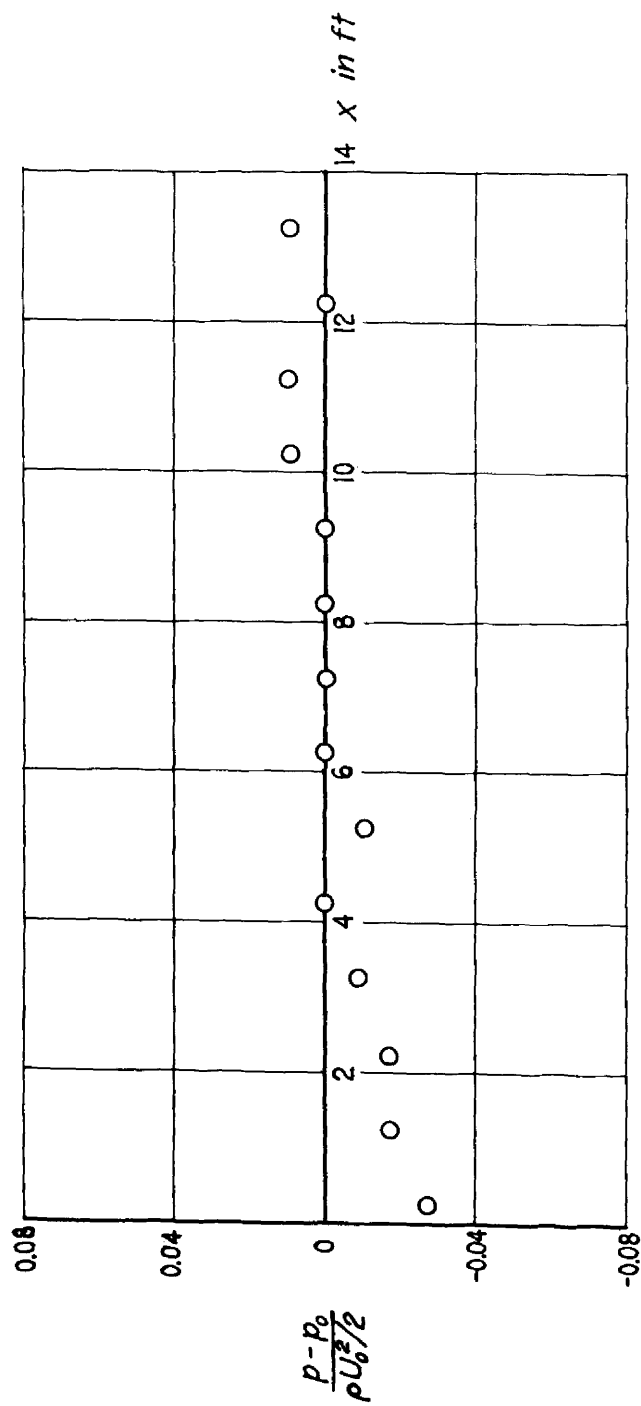


Fig. 1 Plan of wind tunnel



$p_0$  Upstream reference wall pressure

$U_0$  Upstream reference uniform velocity

Fig. 2 Pressure distribution along the centerline of test section

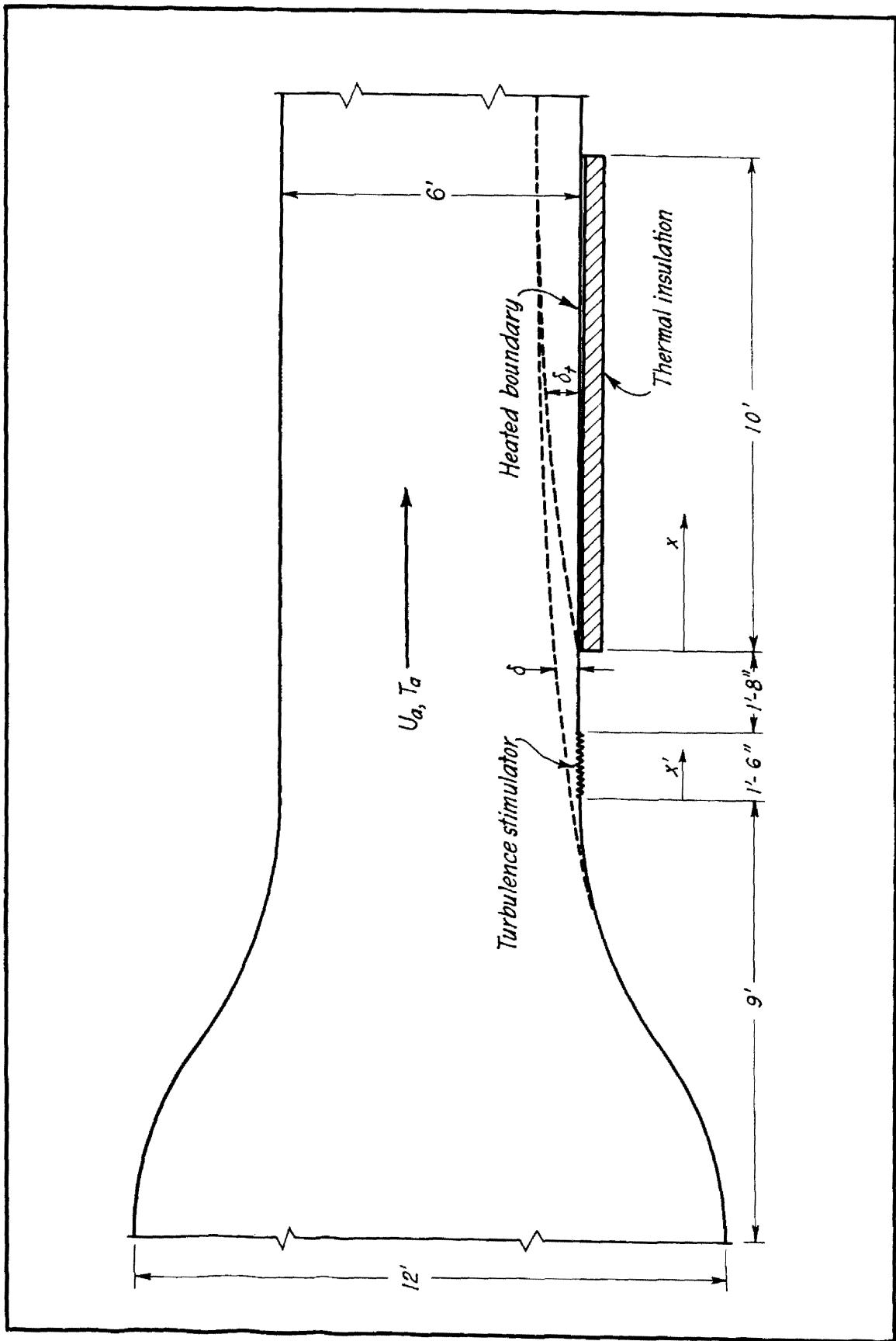


Fig. 3 Schematic diagram of test section

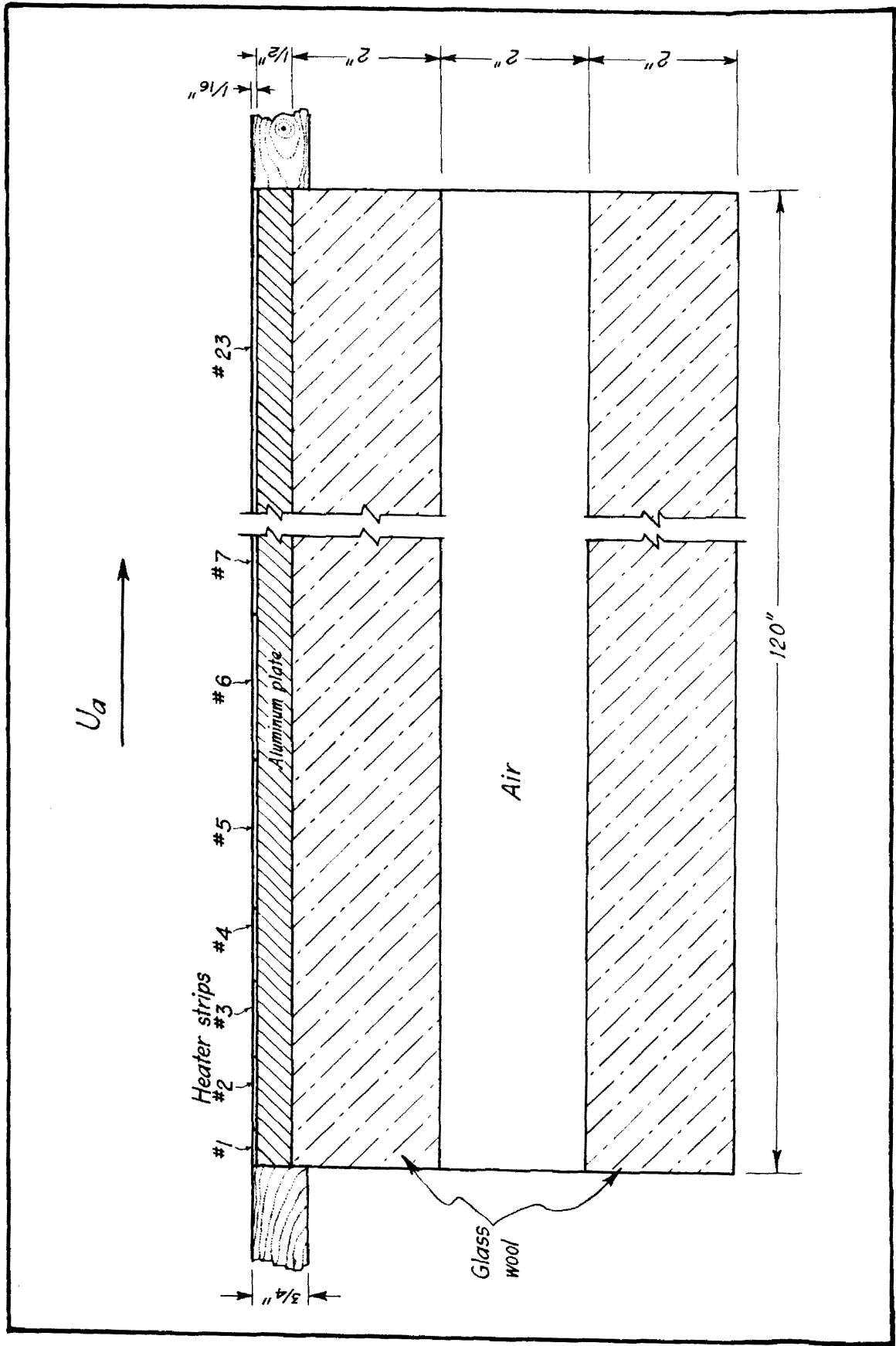


Fig. 4 Heated boundary

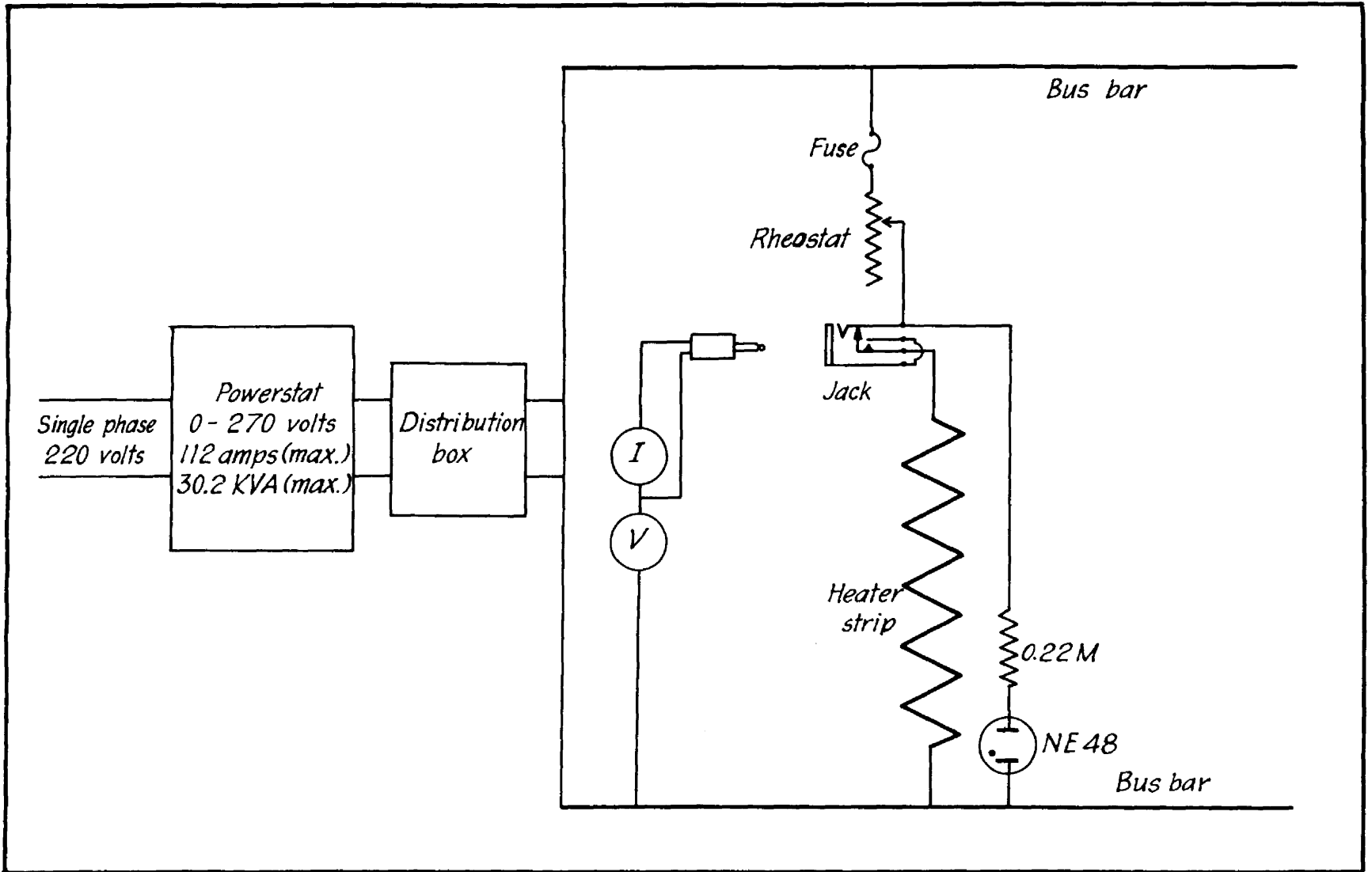


Fig. 5 Circuit diagram of heater strip connections

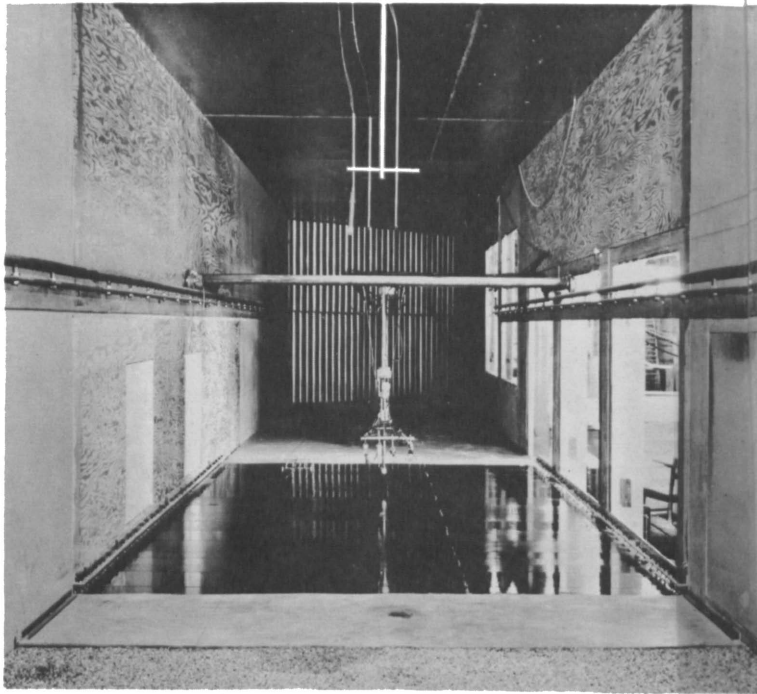


Fig. 6 View of test section looking downstream

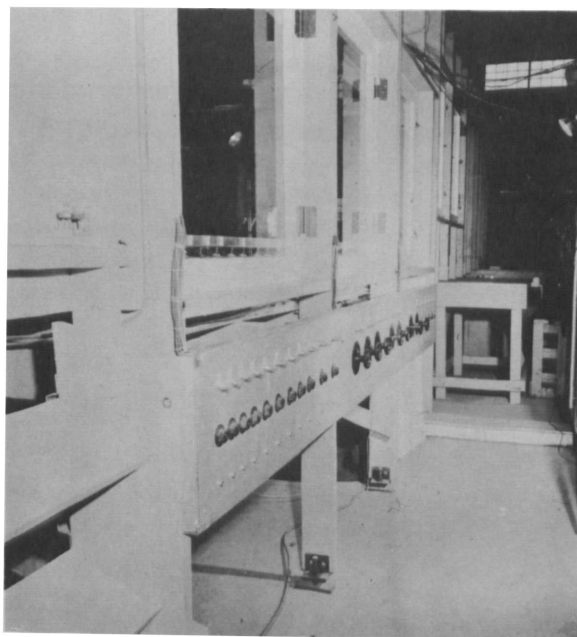


Fig. 7 Electrical control panel of heater strips mounted outside test section



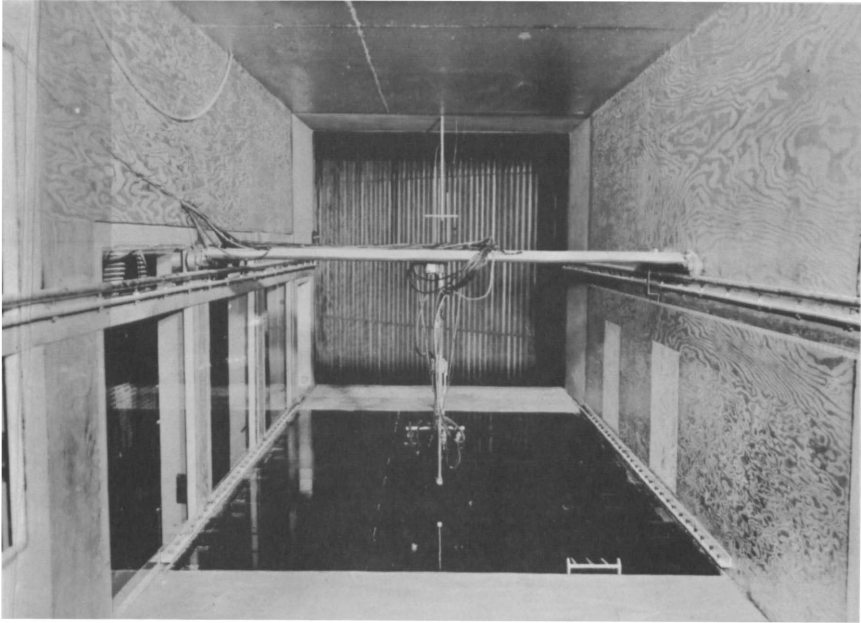


Fig. 8 View of test section looking upstream

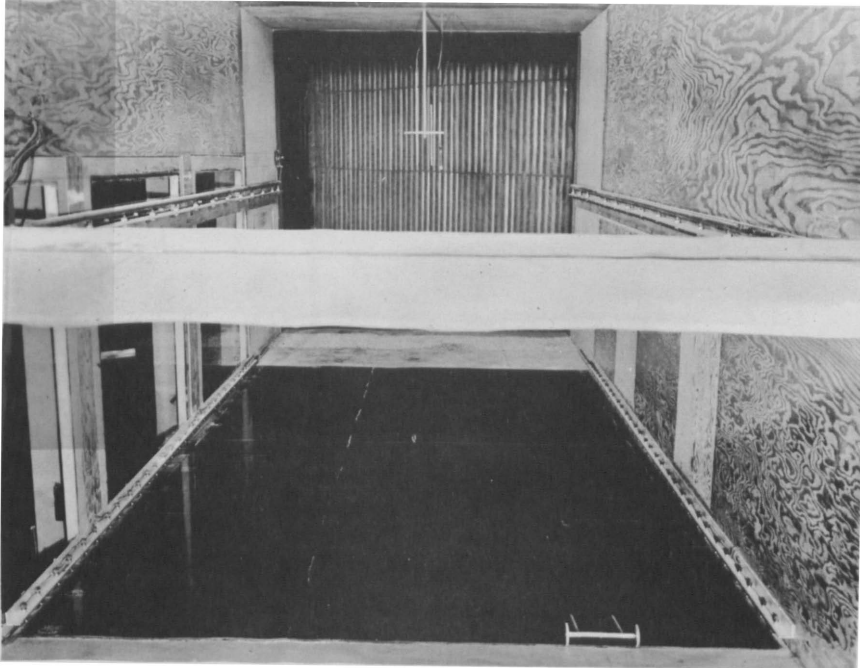


Fig. 9 Close-up view of heated boundary looking upstream.

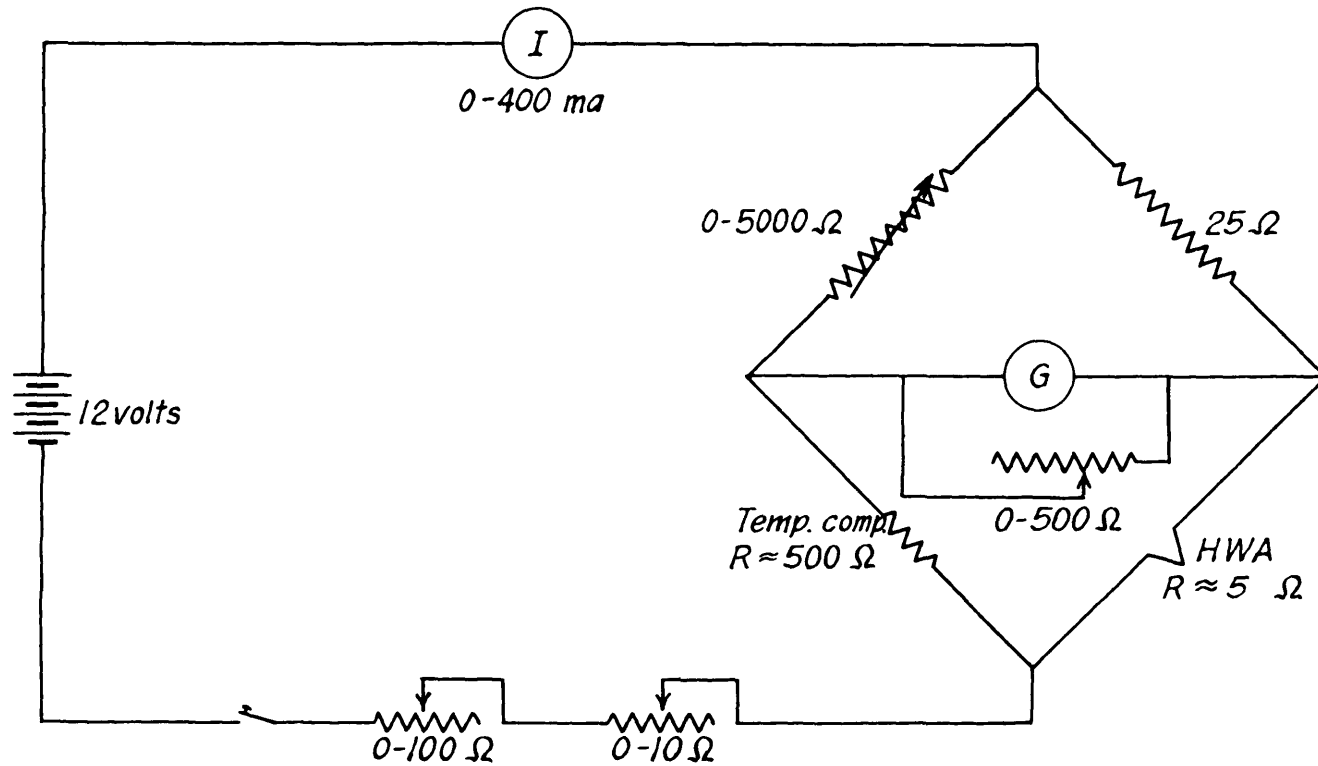
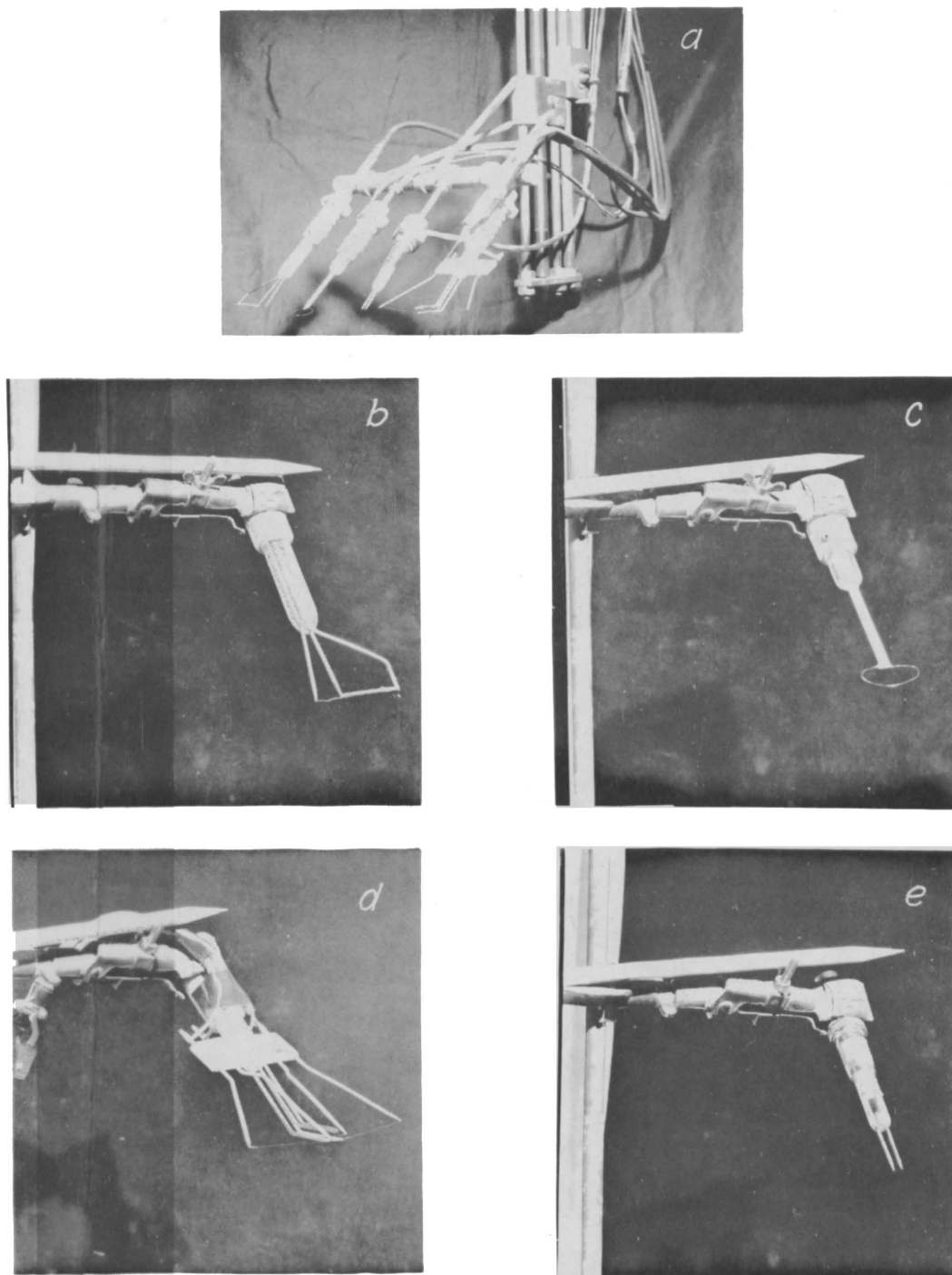


Fig. 10 Constant-temperature hot-wire anemometer for mean velocity



**Fig. 11** Views of probes  
 a Probe assembly  
 b Mean velocity hot-wire probe  
 c Mean temperature thermocouple probe  
 d Turbulence intensities hot-wire probe  
 e Resistance thermometer probe

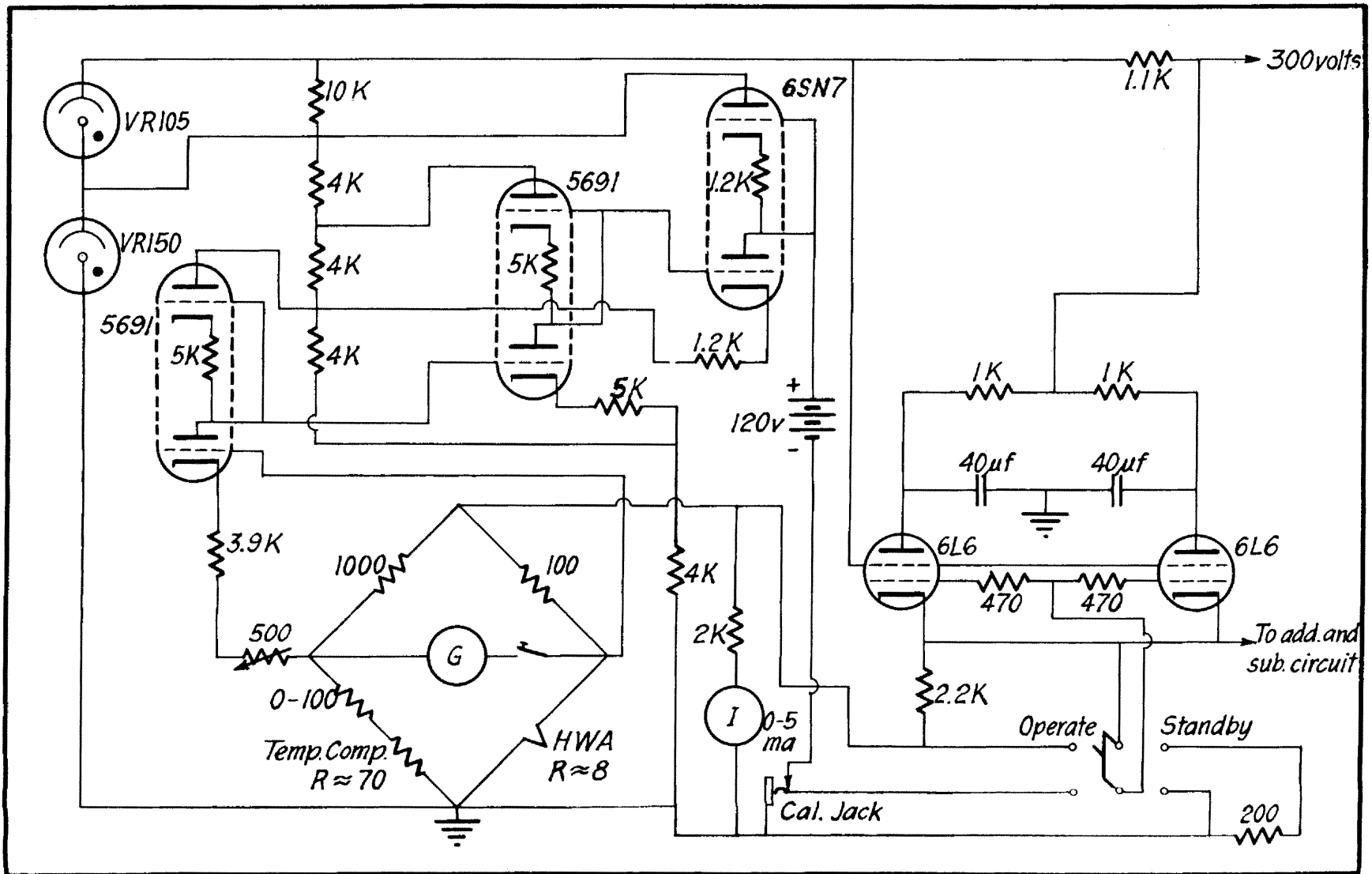


Fig. 12 Constant-temperature, tungsten hot-wire anemometer No. 1 (Current Control Circuit)

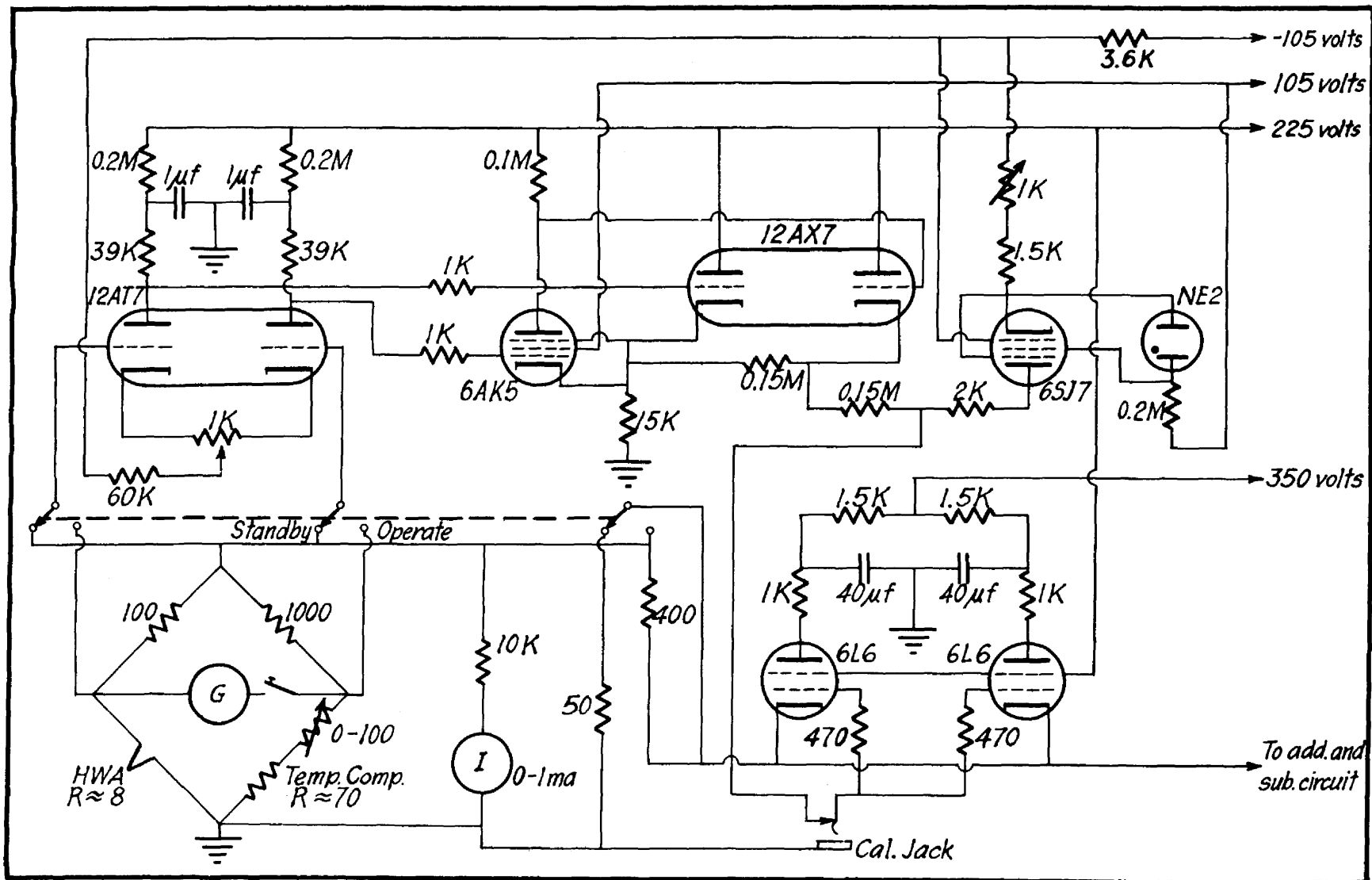


Fig. 13 Constant-temperature, tungsten hot-wire anemometer No. 2 (Current Control Circuit)

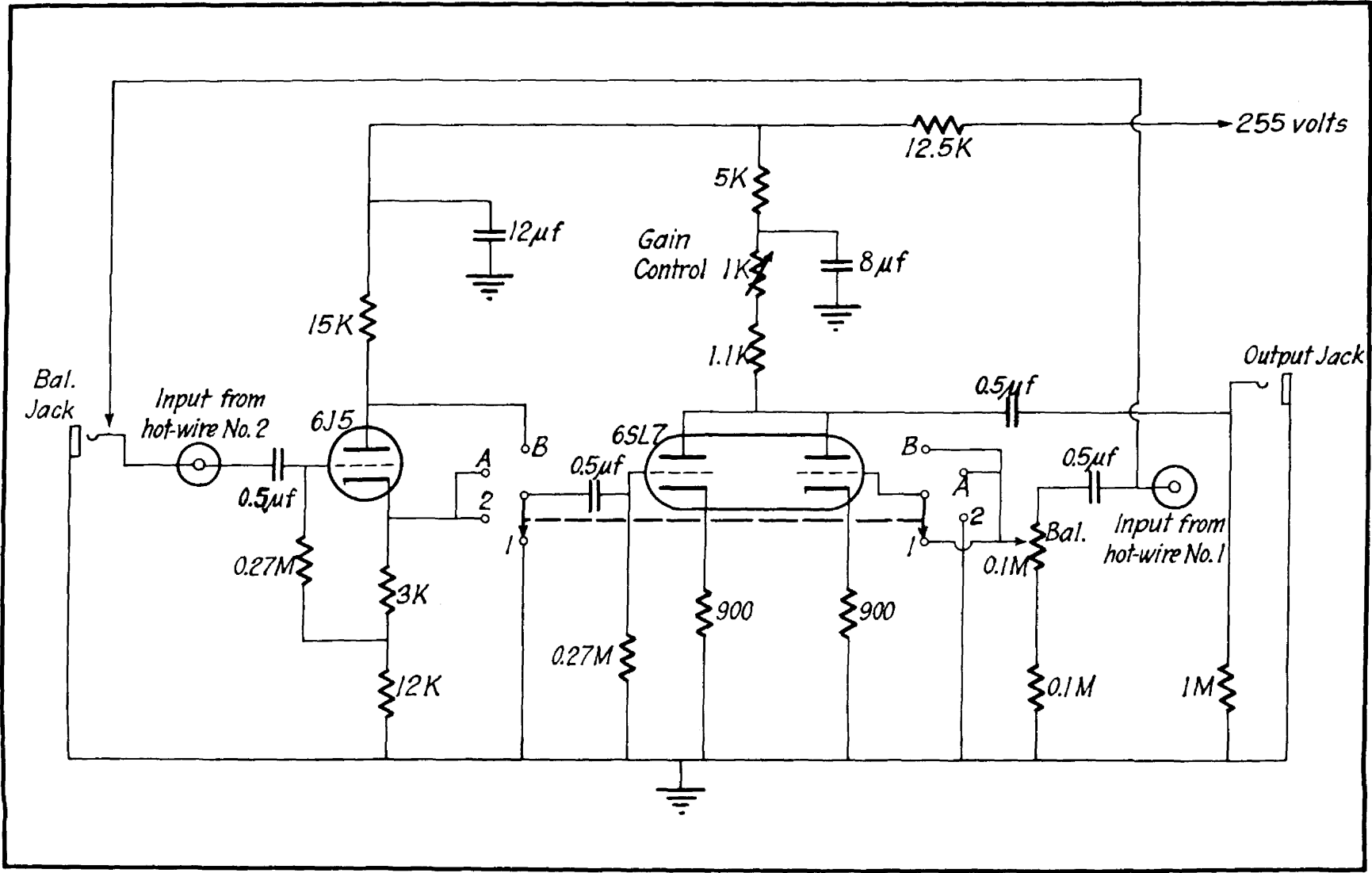


Fig. 14 Adding and subtracting circuit

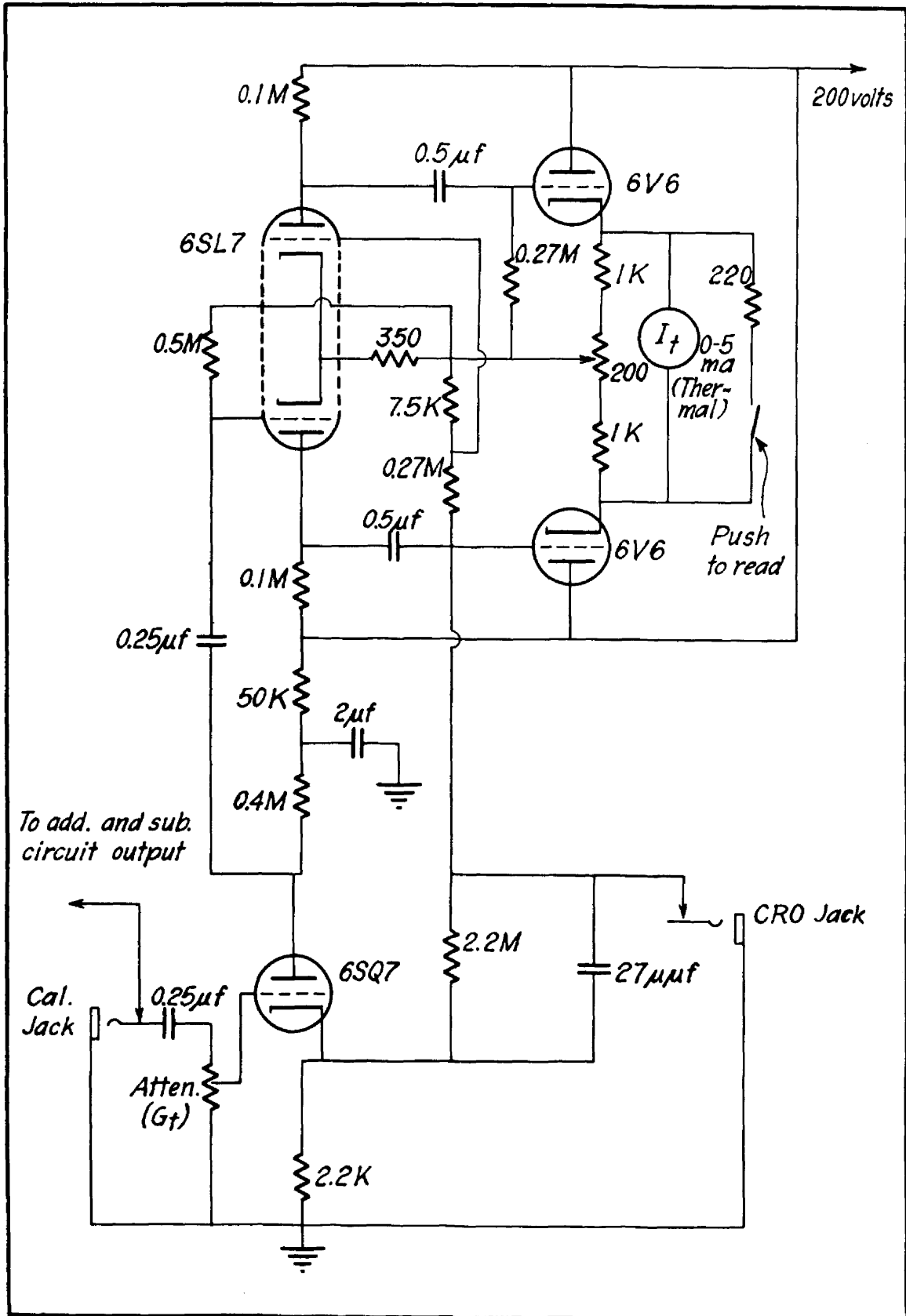


Fig. 15 Turbulence amplifier and RMS indicator circuit

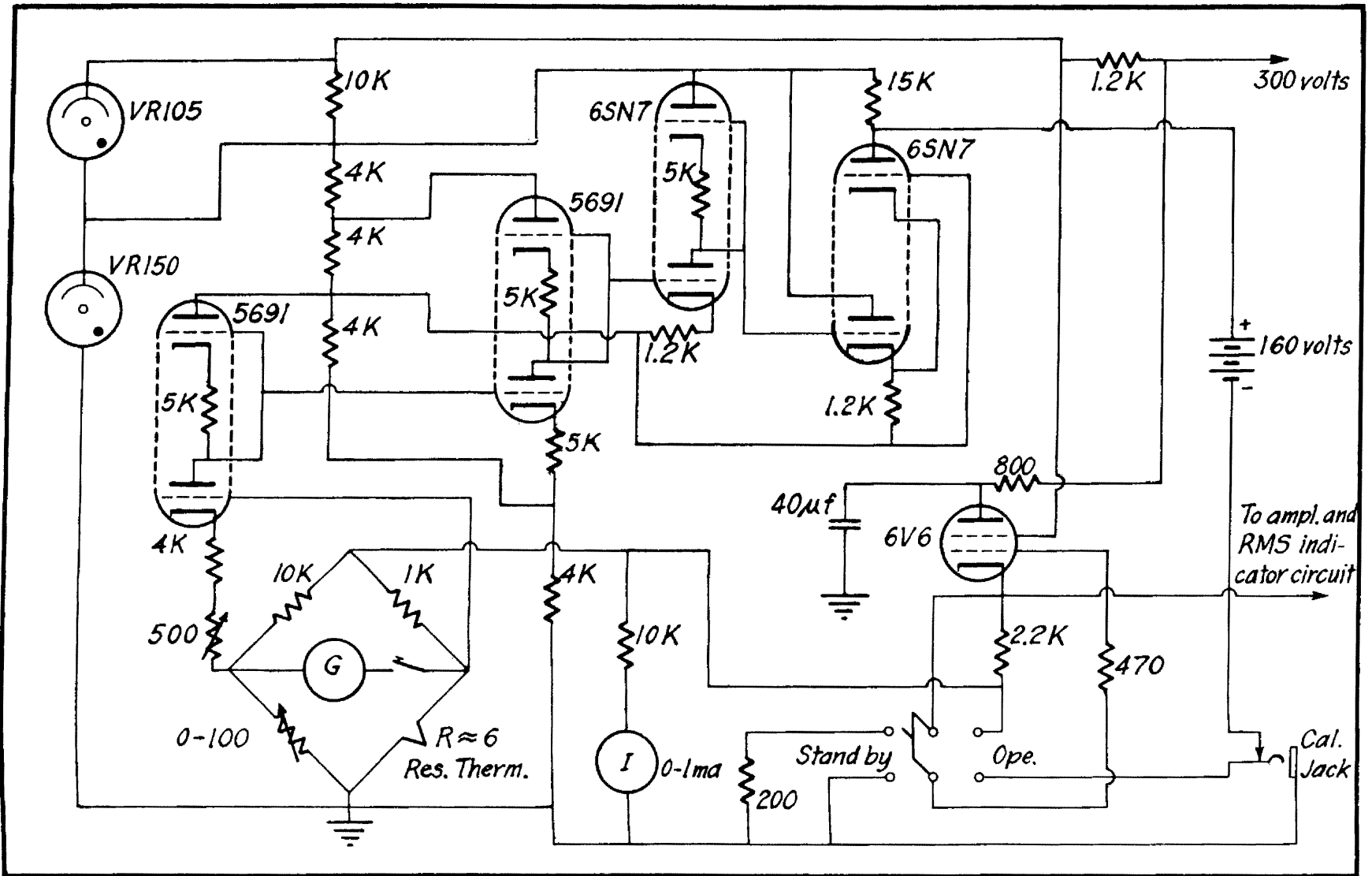


Fig.16 Constant-temperature resistance thermometer (Current Control Circuit)